

05

Experimental and Theoretical Study of high-velocity penetration of long rod projectiles into sand

© S.I. Gerasimov,^{1,2} Yu.F. Travov,¹ A.G. Ioilev,^{1,2} V.V. Pisetsky,² N.N. Travova,² A.P. Kalmykov,¹
S.A. Kapinos,¹ N.V. Lapichev,¹ Yu.I. Faikov¹

¹ Russian Federal Nuclear Center, All-Russia Research Institute of Experimental Physics,
607188 Sarov, Russia

² Sarov Institute of Physics and Technology - National Research Nuclear University MEPhI,
607184 Sarov, Russia

e-mail: SIGerasimov@vniief.ru, YFTravov@vniief.ru

Received October 13, 2021

Revised December 12, 2021

Accepted December 13, 2021

Results of computations with the use of improved modified Alekseevskii–Tate theory (IMATT) are compared to experimental data on high-velocity penetration of long rod projectiles into sand in the impact velocity range of $V_0 = 0.5–3.5$ km/s. Projectiles were made of three different metals: M1 copper, WNZh tungsten heavy alloy and 30KhGSA steel. The value of hardening coefficient k in the linear dependence of the projectile material yield on pressure could be determined using IMATT and experimental data on dependence of differential penetration coefficient K on the penetration velocity. At penetration in regime of the hydrodynamic erosion of projectile, differential penetration coefficient K could be approximated just by dependence on the ratio of the impact velocity of penetration to the value of the critical velocity, above which the projectile deforms plastically during penetration. The values of the critical velocity may differ for specific projectile material properties as well as the density and the humidity of sand.

Keywords: high-velocity penetration, plastic deforming, yield, hydrodynamic erosion, Alekseevskii–Tate theory, experiment.

DOI: 10.21883/TP.2022.03.53261.275-21

Introduction

For describing the process of high-velocity penetration of cylindrical projectile (rod) into sandy soil, the modified hydrodynamic theory (MHT) of Alekseevskii–Tate [1–3] was improved [4], allowing to calculate the process of high-velocity penetration of the projectiles into weak constriction both in hydrodynamic and plastic deforming stages. The following experimental data are used in the improved MHT (IMHT):

— critical velocity V^* (implementation velocity, at which the plastic stage of penetration starts for certain soil parameters);

— pressure coefficient in stagnation point \bar{P}_T ;

— plastic wave propagation velocity in the rod C_p ;

— dependence of the projectile material yield on pressure $Y_p(P)$.

In the work [4] IMHT is used for describing the experimental data on high-velocity penetration of rods of copper M1 into sand. In this work the study also includes penetration of rods, made of VNZh alloy [5] and 30HGSA steel, into sandy soil.

1. Physical scheme of rods deforming at high-velocity implementation into weak constrictions

Three modes of deforming, that are implemented at various movement velocity, exist at high-velocity penetration of the projectiles into dense media [6–8]:

1) „solid body“ mode — projectile deforms elastically; 2) plastic deforming mode — reduction of the projectile length is performed with constant velocity, equal to longitudinal plastic wave velocity C_p ;

3) hydrodynamic actuation mode — projectile actuation velocity $V-U$ exceeds the longitudinal plastic wave velocity (V is velocity of a tail undeformed part of the projectile; U is penetration velocity).

Figure 1 shows the schemes of the cylindrical projectile deforming, corresponding to plastic and hydrodynamic modes. Values of L and L_p are defined as per X-ray image of the projectile in soil at the fixed time of penetration [9].

In Fig. 1, a ΔL_{mr} is value of the plastically deformed front part. It should be noted, that the plastically deformed front part of the projectile is clearly distinguishable for the projectiles of plastic materials only. If projectiles are made of brittle materials (high-strength steels, ceramic compounds, tungsten carbide, etc.), the plastically deformed

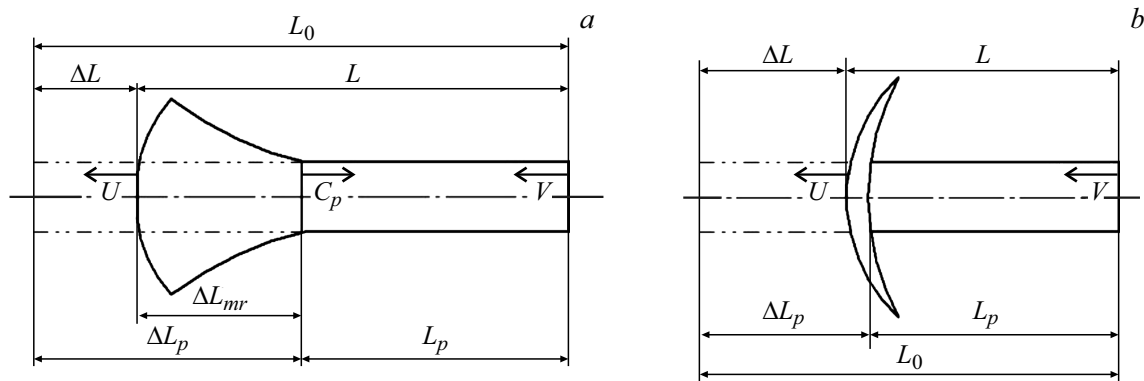


Figure 1. Scheme of the projectile deforming at high-velocity penetration into sand: *a* — plastic deforming mode, *b* — hydrodynamic actuation mode ($\Delta L_p = \Delta L$).

front part can break into pieces, that are removed in radial direction with the constriction material.

If during plastic mode the current projectile length L is equal to its length after complete stagnation in constriction, it means, that, at least from the moment of X-ray radiography and until the stop, the penetration was performed in „solid body“ mode, but the shape of this body is not initial, but plastically deformed at the moment of X-ray radiography.

Projectile penetration is performed at plastic deformation mode, if penetration velocity exceeds some critical value V_* , that can be evaluated using the modified Bernoulli equation [1,2], expressing the pressure balance in critical point from the soil and rod sides:

$$\frac{1}{2} \rho_p (V - U)^2 + Y_p = \frac{1}{2} \bar{P}_T \rho_t U^2 + R_t, \quad (1)$$

where ρ_p and ρ_t are density of metal rod (penetrator) and constriction (target), Y_p is dynamic yield of penetrator material, R_t is dynamic hardness of constriction material. If constriction is a soft soil, the projectile material is stronger than constriction material $R_t \ll Y_p$, therefore the value of R_t compared to Y_p will be neglected further. For consideration of significant compressibility of the soil constriction the pressure coefficient \bar{P}_T is added to the equation (1).

Transition from the mode of projectile penetration as a „solid body“ to the mode of projectile penetration with its plastic deforming corresponds to condition $V = U = V_*$, i.e. the critical penetration velocity is equal to

$$V_*^2 = 2 \frac{(Y_* - R_t)}{\rho_t \bar{P}_T}. \quad (2)$$

In classical MHT (see for instance [3,6]) Y_p is a constant dynamic strength of the projectile, indicating the stress, at exceeding of which the projectile material becomes „liquid“. In equation (1) the dynamic yield of the projectile material Y_p is considered dependent on pressure (velocity) [4], in relation (2) Y_* is the yield at critical velocity V_* .

Value of \bar{P}_T is close to coefficient of resistance C_x of the flat face of cylinder. When using the experimental value of C_x (considering its dependence on soil moisture [10]), there is no need to consider R_t , since it is already considered in the total resistance coefficient.

Penetration is performed in hydrodynamic mode [6], if penetration velocity exceeds velocity of hydrodynamic transition V_{ht} , that is defined as per the equation (1), if the projectile actuation velocity $(V - U)$ is equal to the longitudinal plastic wave velocity C_p .

If longitudinal stress $\sigma_x < 50$ GPa,¹ when temperature influence is not significant yet, the yield of metal can be considered as linearly dependent on implemented pressure [11,12]:

$$Y_p(P) = Y_0 + kP, \quad (3)$$

where k is strengthening coefficient. Pressure in critical point of the projectile P can be evaluated as $P = C_x \rho_t V^2 / 2$. Then, from relation (2) (if $Y_p > Y_*$) it concludes, that $P_* = Y_*$ and, therefore, $Y_* = Y_0 + kY_*$, and expression (3) can be written as

$$Y_p(P) = Y_*(1 - k) + kP. \quad (4)$$

Then, the velocity of hydrodynamic transition is defined from (1) as

$$V_{ht} = \frac{C_p}{1 - k} + \left[V_*^2 + \frac{C_p^2}{(1 - k)^2} \left(k + \frac{1 - k}{C_x \mu^2} \right) \right]^{1/2}, \quad (5)$$

where $\mu = \sqrt{\rho_t / \rho_p}$.

At constant yield of $k = 0$ the expression for velocity of hydrodynamic transition is simplified:

$$V_{ht} = C_p + \left[V_*^2 + \frac{1}{C_x} \left(\frac{C_p}{\mu} \right)^2 \right]^{1/2}.$$

Another two characteristic velocities of implementation into weak constrictions, V_p and V_{sh} , which can be calculated as per IMHT, are of practical interest.

¹ In all experiments, presented in this work, the pressure, appearing at projectiles penetration into sandy soil, does not exceed ≈ 25 GPa.

Velocity V_{sh} is a minimum implementation velocity in hydrodynamic mode ($V_{sh} > V_{ht}$), at which the complete hydrodynamic actuation of the projectile is performed at the moment of its braking to the hydrodynamic transition velocity V_{ht} .

Velocity V_p is a minimum implementation velocity, at which the projectile is plastically deformed completely, i.e. either be completely compressed to a length $L = \Delta L_{mr}$, reaching at braking the critical velocity V_* (case of „soft“ metal in plastic deforming stage), or be completely destroyed (case of brittle metal).

At implementation velocity $V_0 < V_p$, there is always a solid residue of projectile, that continues to move in „solid body“ mode. This penetration mode is not examined in this work. Velocity V_p can be less or more than the hydrodynamic transition velocity V_{ht} . In the latter case at impact velocity $V_p > V_0 > V_{ht}$ the penetration is initially performed in the mode of the projectile hydrodynamic actuation, and then in the mode of its plastic deforming and, at last, in „solid body“ mode. Situation, when $V_p > V_{ht}$, exists in case of relatively small difference of critical velocity V_* from hydrodynamic transition velocity V_{ht} , that, in its turn, is defined with the plastic wave velocity C_p and rather high value of V_* .

One of the main parameters, characterizing the high-velocity interaction of projectile with constriction, is a relative penetration coefficient $K = h/\Delta L$ (h is current implementation depth; ΔL is projectile shortening (actuation)). Coefficient K allows to predict the full depth of the projectile actuation at penetration in hydrodynamic mode. As per Alekseevskii–Tate scheme [1,2], the value of K depends on implementation velocity V . With V increase the value of K decreases, reaching the asymptotic value, defined with formula of M.A. Lavrentiev [13] for the case of ideal incompressible liquid:

$$K = \sqrt{\rho_p/\rho_t}.$$

Along with coefficient K another dimensionless coefficient is examined — deforming coefficient $K_p = h/\Delta L_p$ (ΔL_p is shortening of hard (undeformed) part of the projectile due to plastic deforming). In hydrodynamic mode due to insignificant (compared to the projectile length) thickness of the projectile material liquid phase at contact boundary $\Delta L = \Delta L_p$, i.e. $K_p = K$. In the work [4] it is shown (at least for copper+sand pair), that for velocities V , higher than minimum velocity of total plastic deforming ($V > V_p$), but lower than hydrodynamic transition velocity V_{ht} , the value of K_p also does not depend on the current penetration depth. Under the specified conditions the coefficients K and K_p slightly differ from initial ones:

$$K_p = K_{p0} = \frac{dh}{d(\Delta L_p)} = \frac{U_0}{C_p}, \quad (6)$$

$$K = K_0 = \frac{dh}{d(\Delta L)} = \frac{U_0}{V_0 - U_0}, \quad (7)$$

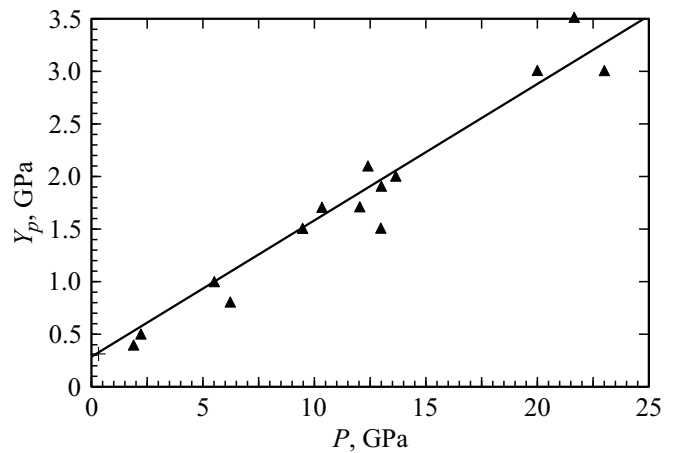


Figure 2. Dependence of copper yield on pressure. \blacktriangle — experiment ([4], copper M1); $+$ (in the lower left corner) — start of plastic stage of deforming: $Y_p = Y_* = 0.320$ GPa; — — $Y_p = Y_*(1-k) + kP$, at $k = 0.13 \pm 0.004$.

where U_0 is defined from (1) considering dependence of $Y_p(V_0)$.

In the work [4] the process of rod of copper M1 (yield — $\sigma_{0.2} \approx 0.290$ GPa, density — $\rho_p = 8.9$ g/cm³) penetration to sand (density — $\rho_t = 1.7$ g/cm³, moisture — $W \approx 10\%$, resistance coefficient — $C_x = 1.5$) is studied in detail. Experimental data from [11] were used for observing the dependence of yield $Y_p(P)$. Figure 2 shows the experimental data of $Y_p(P)$ [4] and their linear approximation with expression (3) for determination of the strengthening coefficient k . The following is observed based on results of experiments and calculations as per IMHT: $V_* = 0.500$ km/s; $k = 0.13$; $Y_* = 0.320$ GPa; $V_p = 0.850$ km/s; $V_{ht} = 1520$ m/s; $V_{sh} = 2.100$ km/s.

For calculation of copper projectile penetration as per IMHT the dependence of the projectile material yield (in a range of $P \leq 25$ GPa) was defined according to expression (4), as per the following formula:

$$Y_p(V) = Y_*(1 - k) + kC_x\rho_t V^2/2. \quad (8)$$

It is assumed, that pressure is the function of the hard (undeformed) projectile part movement velocity. Approach in selection of pressure evaluation method in the yield formula (8) is taken based on the following considerations. At high-velocity penetration of the projectile into the continuous medium the pressure at the contact boundary is $P = \rho_t C_x U^2/2$ and, correspondingly, considering the linear dependence of yield on pressure (3), the expression for yield calculation should be nominally the following

$$Y_p(U) = Y_0 + k_1 C_x \rho_t U^2/2, \quad (9)$$

where coefficient k_1 is implemented for consideration of the projectile deforming non-unidimensionality. In experiments on projectiles penetration into constrictions the only known

Table 1. Experiments with projectiles of copper M1 at penetration into sand [4]

Plastic mode													
V_0 , km/s	Experimental data							Calculation as per IMHT					
	h , mm	t_p , μ s	ΔL , mm	ΔL_p , mm	$K_p = h/\Delta L_p$	$K = h/\Delta L$	$C_p = \Delta L_p/t$, m/s	t , μ s	ΔL , mm	ΔL_p , mm	$K_p = h/\Delta L_p$	$K = h/\Delta L$; δ , %	
0.703	27.5	44.2	5.5	20.0	1.37	5.00	452	48.1	5.7	21	1.31	4.82 (-3.6)	
0.853	70.0	96.8	19.0	42	1.67	3.68	434	109.4	19.3	47.8	1.46	3.63 (-1.4)	
0.879	65.0	93.8	20.0	41	1.58	3.25	437	98.9	18.7	43.2	1.51	3.48 (7.0)	
0.965	62.0	81.9	19.5	35	1.77	3.18	427	87.4	19.7	38.2	1.62	3.15 (-1.0)	
1.080	57.0	67.8	19.0	30	1.90	3.00	442	72.9	19.3	31.8	1.79	2.95 (-1.7)	
1.125	53.0	61.0	18.0	27	1.89	2.94	443	65.3	18.9	28.5	1.86	2.80 (-4.8)	
1.214	125	136	48.0	58	2.15	2.60	426	149.4	45.3	65.3	1.91	2.76 (6.1)	
1.218	120	141	45.0	60	2.00	2.67	426	142.5	43.7	62.2	1.93	2.75 (3.0)	
1.225	90	96	32.0	42	2.14	2.81	438	104.4	33.2	45.6	1.97	2.71 (-3.6)	
1.330	102	104	38.5	46	2.21	2.65	442	110.3	39.0	48.2	2.12	2.62 (-1.1)	

Hydrodynamic mode								
V_0 , km/s	Experimental data				Calculation as per IMHT			
	h , mm	t_p , μ s	ΔL , mm	$K = h/\Delta L$	t , μ s	ΔL , mm	$K = h/\Delta L$; (δ %)	
1.544	105	104	44	2.39	98.8	42.3	2.48 (3.8)	
1.590	155	153	62	2.50	145.3	62.4	2.48 (-1.0)	
1.636	65	58.4	28	2.32	57.0	26.7	2.43 (4.7)	
1.639	63	60	25	2.52	55.2	25.9	2.43 (-3.6)	
1.650	105	97	42	2.50	92.8	43.0	2.44 (-2.4)	
2.000	125	102	52	2.40	92.5	53.2	2.35 (-2.0)	
2.006	135	110	58	2.33	100.2	57.4	2.35 (1.0)	

variables are initial implementation velocity V_0 and density of constriction and projectile ρ_t and ρ_p . Therefore, in formula (9) the transition from penetration velocity U to hard projectile part movement velocity V has been made using their relation in hydrodynamic approximation: $U = V/(1 + \mu)$ [13]. In our case the coefficient μ considers the compressibility of the soil constriction:

$$\mu = \sqrt{C_x \rho_t / \rho_p}. \tag{10}$$

Then, as with expression (4), the dependence of yield on velocity can be written as

$$Y_p(V) = Y_* \left[1 - \frac{k_1}{(1 + \mu)^2} \right] + \frac{k_1}{(1 + \mu)^2} C_x \rho_t V^2 / 2. \tag{11}$$

Value of $(1 + \mu)^2$ is defined by density of projectile and constriction and resistance coefficient.

For determination of the coefficient k_1 value the experimental data on relative penetration coefficient K at copper projectile movement in sandy soil, observed at various initial velocities $V_0 > V_p$ (Table 1), were used. Using the equation (1) and assuming K stationary at implementation velocity of $V_0 > V_p$, the following expanded form can be written

$$K(V) = \frac{dh}{d(\Delta L)} = K(V_0) = \frac{U_0}{V_0 - U_0} = \sqrt{\frac{\rho_p}{C_x \rho_t}} \sqrt{\frac{1}{1 - \frac{2Y_p(V_0)}{C_x \rho_t U_0^2}}}. \tag{12}$$

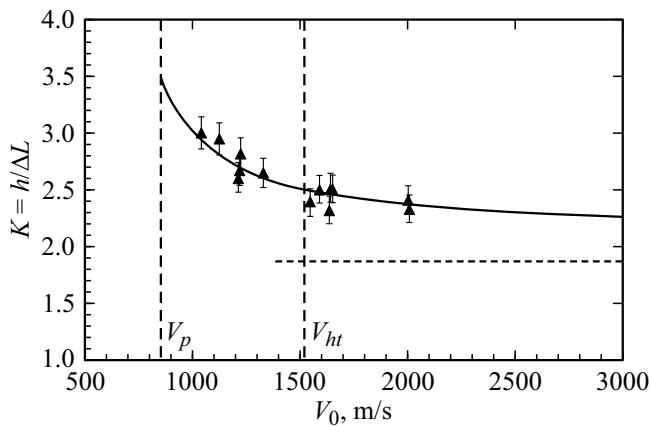


Figure 3. Experimental values of the relative penetration coefficient K of the copper projectile in sand. \blacktriangle — experiment (Table 1, scatter $\pm 5\%$); — — approximation with analytical dependence (10), $Y_p = Y_p(V)$ considering (8), (11) with coefficient $k = 0.128$, $Y_* = 0.320$ GPa ($V_* = 500$ m/s).

For determination of coefficient k_1 let's use the formula (11) for yield $Y_p(V)$ in the equation (1) at $U = U_0$:

$$U_0 = \frac{V_0}{1 - \mu^2(1 - k_1)} \times \left[1 - \sqrt{1 - (1 - \mu^2(1 - k_1)) [1 + (1 - k_1)\mu^2 V_*^2 / V_0^2]} \right]. \quad (13)$$

Approximation of experimental data with the least squares method by relative penetration coefficient K of the copper projectile using the expression (10f) considering (11) and (13) results in $k_1 = 0.302 \pm 0.005$ (calculated mean-square deviation is presented). In case of copper projectile penetration into sand the value of the coefficient (10) $\mu = 0.535$, then the value of strengthening coefficient (11) $k = k_1 / (1 + \mu)^2 = 0.128 \pm 0.002$. Approximating dependence of the relative penetration coefficient of the copper projectile is shown in Fig. 3. The observed value $k = 0.128 \pm 0.002$ is almost equal to the value of the strengthening coefficient $k = 0.13 \pm 0.004$, calculated as per data of direct experiments with plane shock wave (Fig. 2). Thus, replacement of velocity U with V during evaluation of implemented pressure allows to apply the expression (8) for calculation of the projectile material yield, using the value of the strengthening coefficient k , observed from direct experiments of $Y(P)$ determination. In this case the expression (13) for penetration velocity, considering the dependence of yield as per formula (8), will be the following:

$$U_0 = \frac{V}{1 - \mu^2} \left[1 - \mu \sqrt{1 - (1 - \mu^2)[k + (1 - k)V_*^2 / V_0^2]} \right]. \quad (14)$$

2. Experimental set up

Application of IMHT [4] for copper M1 was based on coefficients of dependence $Y_p(P)$, known from [11]. We don't know such dependence for VNZh tungsten alloy and 30HGSA steel, and exactly this circumstance was the reason behind determination of $Y_p(P)$ for these metals as per to results of experiments on high-velocity penetration of cylindrical projectiles of VNZh alloy and 30HGSA steel. Experiments on studying the process of metal projectiles penetration into soil were performed using missile ballistic units [14]: at missile velocities of up to 1.5 km/s the powder unit was used, for higher missile velocities — two-stage light-gas units.

Figure 4, *a* shows the experimental set up scheme [9,15,16]: 1 — recorder, 2 — coils, 3 — magnets, 4 — barrel ballistic unit, 5 — container with sand, 6 — „EPOS“ camera or X-ray apparatus (XRA) „Argument-120“, 7 — XRA „Argument-120“. Registration of the projectile position before entering into soil was performed with XRA „Argument-120“ or „EPOS“ photooptic system, while registration of the projectile, moving in soil, was performed using XRA „Argument-120“ [9].

Figure 4, *b* shows the picture of the projectile of VNZh alloy in air before entering into the container with sand. Behind are the leafs of duralumin tray, flying to the side, in front is the vertical line — dropper, acting as a plumb, that allows to evaluate the possible initial angle of attack.

Container, filled with sand, with a width of 5–10 cm, depending on the penetrating projectile diameter, was used as soil constriction. In experiments the fine-grained sand with density and moisture in a range of $\rho_t \approx (1.6–1.8)$ g/cm³ and $W \approx (8–12)\%$ was generally used. In five experiments with projectile of VNZh alloy [5] the sand was almost dry. Rod projectiles of copper M1, VNZh alloy and 30HGSA steel had front face diameter of $d_k \approx 4–11$ mm, length of $L_0 = 30–80$ mm, and weight of $m = 7–60$ g.

Experimental data, including actual parameters of sandy soil and projectiles, are presented in Tables 1–3. These tables also contain the values, calculated as per IMHT, comparison with experimental data was performed for values of V_0 and h of individual experiments. Value of plastic wave velocity is presented in Table 4. The initial data for calculation as per IMHT are the following:

— experiments [4] with projectiles of copper M1 (Table 1): average values of soil parameters: $\rho_t = 1.7$ g/cm³, $W = 10\%$ ($Y_* = 0.320$ GPa, $k = 0.13$; $C_x = 1.5$), projectile parameters: $d = 10$ mm, $m = 57.5$ g, $\rho_p = 8.9$ g/cm³, $\sigma_{0.2} \approx 0.290$ GPa;

— experiments with projectiles of 30HGSA steel (Table 2): $Y_* = 1.34$ GPa, $k = 0.175$, projectile parameters: $d_m = 22.5$ mm, $\rho_p = 7.85$ g/cm³, $\sigma_t \approx 1.100$ GPa (medium-strength steel [17]);

— experiments with projectiles of VNZh alloy (Table 3) [5]: $Y_* = 1.775$ GPa, $k = 0.25$, $\rho_p = 17.0$ g/cm³, values of mass m and diameter d of projectile are presented in the table, $\sigma_t \approx 0.877$ GPa [5].

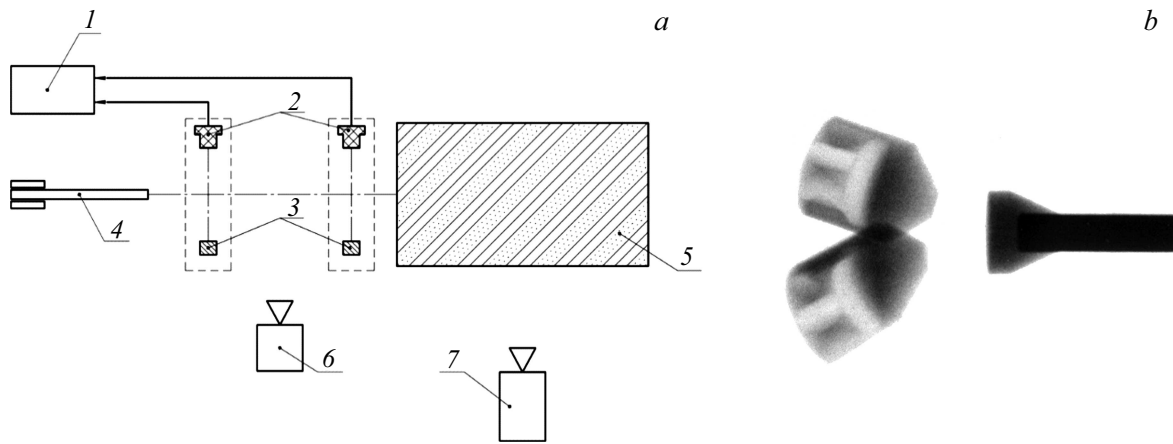


Figure 4. Scheme of experiments performing (a) and projectile of VNZh alloy during flight (b).

Table 2. Experiments with projectiles of 30HGSA steel at penetration into sand

Item No.	V_0 , km/s	m , g	d_k , mm	ρ_t , g/cm ³	W , %	h , mm	ΔL , mm	t_p , μ s	$K = h/\Delta L$	C_x	Calculation as per IMHT		
											ΔL , mm	t , μ s	K ($\delta\%$)
Plastic mode													
1	1.928	60.0	11.25	1.76	9.6	51.0	17.0	34.7	3.0	1.5	15.8	35.8	3.23 (7)
2	1.963	60.0	11.25	1.85	12	37.0	12.0	23.8	3.1	1.4	11.6	25.3	3.19 (3)
3	1.969	60.0	11.25	1.78	9.6	72.0	24.0	50.7	3.0	1.5	22.7	50.4	3.17 (5)
Hydrodynamic mode													
4	2.293	60.0	11.25	1.85	9.0	45.0	16.0	24.7	2.81	1.5	16.4	27.5	2.74 (-2)
5	2.358	60.0	11.25	1.80	10	60.0	22.0	34.5	2.73	1.5	21.8	35.8	2.75 (1)

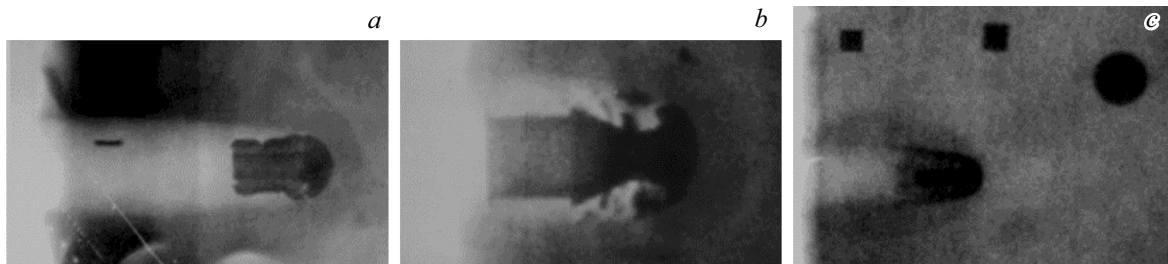


Figure 5. Characteristic X-ray photographs at penetration into sandy soil: a — projectile of copper M1 ($d = 10$ mm, $L_0 = 82.2$ mm), $V_0 = 1.214$ km/s, $\rho_t = 1.7$ g/cm³; b — projectile of 30HGSA steel ($d_k = 11.25$ mm, $d_m = 22.5$ mm, $L_0 = 60$ mm), $V_0 = 1.928$ km/s, $\rho_t = 1.8$ g/cm³; c — projectile of VNZh alloy ($d = 4$ mm, $L_0 = 30$ mm), $V_0 = 3.570$ km/s, $\rho_t = 1.66$ g/cm³.

Experimental penetration depth h , worn ΔL and deformed (for copper rod) ΔL_p part of the projectile are observed by procession of X-ray photographs of penetration process at the point in time t_p [9]. Figure 5 shows the characteristic X-ray photographs of the process of penetration into sand for projectiles of copper M1, 30HGSA steel (d_m is midsection diameter) and VNZh alloy.

Experimental values of the resistance coefficient, presented in Tables 1–4, have mean-square deviation of at

least (2–3)% [10] (considering the error of sand parameters determination). The total error of experimental C_x determination may reach 10%.

3. Measurement results

The following is directly measured in experiments:

- ρ_t — sand density;
- W — sand moisture content by weight;

Table 3. Experiments with projectiles of VNZh alloy at penetration into sand [5]

Item No.	V_0 , km/s	m , g	d_k , mm	ρ_t , g/cm ³	W , %	h , mm	ΔL , mm	t_p , μ s	$K = h/\Delta L$	C_x	Calculation as per IMHT		
											ΔL , mm	t , μ s	K ($\delta\%$)
Plastic mode													
1	1.560	25.85	7	≈ 1.7	≈ 10	55.0	6.2	39.2	8.87	1.5	6.5	41.5	8.46 (–5)
2	1.840	24.10	7	≈ 1.7	≈ 10	57.1	11.9	37.5	4.80	1.5	9.8	38.0	5.8 (20)
3	1.950	24.05	7	≈ 1.7	≈ 10	63.4	14.5	39.8	4.37	1.5	11.7	40.4	5.41 (28)
4	2.000	24.25	7	≈ 1.7	≈ 10	87.1	17.5	54.1	4.98	1.5	16.1	55.3	5.4 (8)
Hydrodynamic mode													
5	2.520	24.05	7.04	1.6	1.4	36.1	9.5	17.7	3.80	2.0	9.6	18.6	3.76 (–1)
6	2.590	7.75	4.06	1.76	11.3	60.6	15.8	29.9	3.85	1.5	14.5	30.1	4.17 (8)
7	2.600	7.70	4.05	1.725	8.2	47.5	12.8	23.4	3.71	1.65	12.0	23.6	3.96 (7)
8	2.620	7.75	4.02	1.825	10.9	36.0	9.0	16.8	4.0	1.5	8.91	17.5	4.04 (1)
9	2.650	7.75	4.01	1.835	11.2	62.7	17.2	30.3	3.65	1.5	15.5	30.8	4.04 (10)
10	3.370	24.25	7.02	1.66	1.55	31.1	8.7	12.6	3.57	2.0	9.2	12.2	3.38 (–5)
11	3.370	24.25	7.05	1.77	10.8	42.4	11.5	15.8	3.68	1.5	11.3	16.2	3.75 (2)
12	3.380	24.10	7.025	1.56	0.6	58.7	16.6	22.2	3.53	2.0	16.9	23.2	3.47 (–2)
13	3.400	7.70	4.04	1.72	8.6	57.3	15.6	21.2	3.67	1.6	15.5	22.1	3.70 (1)
14	3.490	7.7	4.05	1.64	1.1	47.3	13.1	16.7	3.61	2.0	14.1	18.1	3.36 (–7)
15	3.570	7.50	3.96	1.66	0.8	43.8	13.2	15.8	3.32	2.0	13.2	16.4	3.32 (0)

Table 4. Values of average soil parameters, under which the evaluation of the strengthening coefficient k was performed, values of Y_* and C_p at calculation of the projectiles penetration as per IMHT (results in Tables 1–3)

Projectile material	ρ_p , g/cm ³	V_* , km/s (soil parameters)	Y_* , GPa	Average values			k	HB , GPa	C_p , km/s
				C_x	ρ_b , g/cm ³	W , %			
Copper M1	8.9	0.500 [4] ($\rho_t = 1.7$ g/cm ³ , $W = 10\%$, $C_x = 1.5$)	0.32	1.5	1.7	10	0.13	–	0.437
VNZh90 alloy	17.0	1.180 [5] ($\rho_t = 1.7$ g/cm ³ , $W = 10\%$, $C_x = 1.5$)	1.775	1.75	1.7	7.0	0.25	2.365 [5]	0.346
30HGSA steel	7.85	1.000 ($\rho_t = 1.8$ g/cm ³ , $W = 10\%$, $C_x = 1.5$)	1.34	1.5	1.8	10	0.175	2.20 [17]	0.492

— C_x — resistance coefficient of the flat face of the rod (in specially conducted experiments [10]);

— V_0 — initial velocity of implementation into constriction;

— h — current penetration depth as per X-ray photograph;

— t_p — time point of X-ray radiography from the projectile contact with a front surface of soil constriction to X-ray apparatus actuation;

— V_* — critical velocity of penetration (defined in series of the single-type experiments by means of increase of velocity of penetration into sandy soil with certain parameters of density and moisture);

— ΔL , ΔL_p — projectile shortening ($\Delta L = L_0 - L$) and hard projectile part shortening due to plastic deforming ($\Delta L_p = L_0 - L_p$) (Fig. 1).

Value L_p is counted from the back end of the cylinder to the longitudinal plastic wave front, position of which is defined by the projectile cross section with minimum

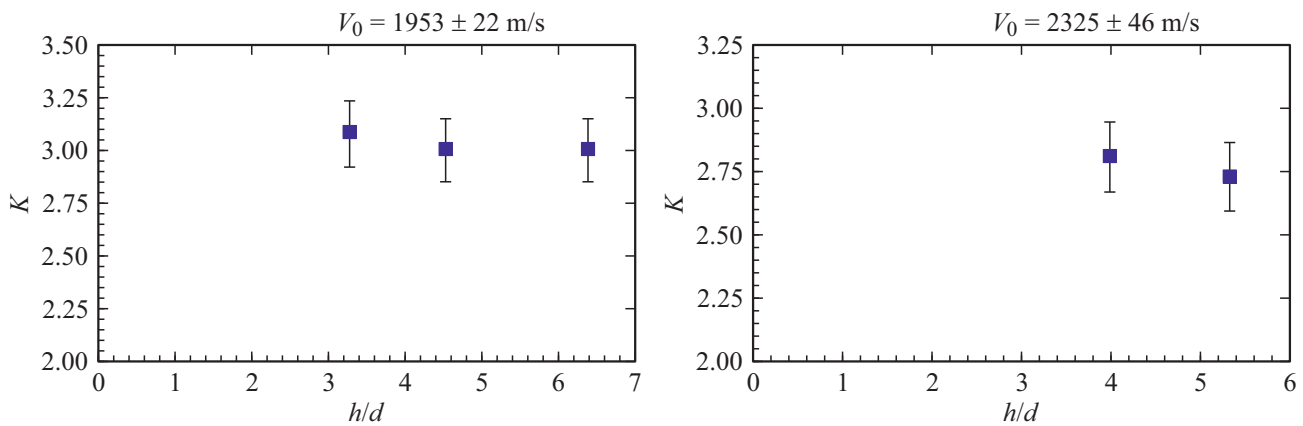


Figure 6. Dependence of relative penetration coefficient on depth of penetration into sand for projectile of 30HGSA steel. ■ — experiment (Table 2, scatter ±5%).

increase of the rod diameter compared to the initial one (in our experimental studies the diameter increase of up to 10% was examined).

Table 4 includes the observed experimental values of V_* at certain sand parameters, average values of ρ_t , W and C_x for several performed experiments, when approximation of experimental dependencies of $K(V_0)$ was performed to define the strengthening coefficient k for this metal. Table 4 also includes values of Y_* , defined directly from formula (2), based on experimentally observed value of V_* , projectile density material ρ_p , strengthening coefficient k , defined with approximation of the experimental dependence $K(V_0)$ by expression (10), value of Brinell hardness of projectile material HB and C_p — velocity of longitudinal plastic wave for this metal.

Velocity of longitudinal plastic wave in experiments with copper projectile [4] is defined from the experiments by measurement of undeformed rod part L_p as per X-ray photographs and time t of penetration process registration. Value of C_p for VNZh alloy and 30HGSA steel was evaluated theoretically. The empirical formula, using material Brinell hardness, was proposed in work [7] based on experiments with sufficiently strong metals for evaluation of longitudinal plastic wave velocity:

$$C_p = \sqrt{\frac{0.863 \cdot HB}{\rho_p}}$$

For 30HGSA the hardness value of $HB = 2.20$ GPa is taken[17]. For VNZh alloy the hardness value of $HB = 2.365$ GPa is taken[5], that was measured at samples, from which the projectiles were turned.

4. IMHT equations system. Determination of strengthening coefficient

Classical MHT equations system, describing the penetration process, was complemented with equations for plastic deforming stage, while value of Y_p (as dynamic yield of

projectile material [1]) is taken as dependent on penetration velocity [4]. Penetration in „solid body“ mode is not examined in this work: hard projectile part velocity V can change from V_0 to V_* . Within this process the projectile material yield will also change. As was stated above, the compressibility of sandy soil was also considered through the resistance coefficient C_x of the flat face.

Full equations system, describing the penetration process both in plastic and hydrodynamic deforming stages considering expressions (1), (2), (5), (8), is the following [4]:

$$\frac{dh}{dt} = U, \tag{15}$$

$$\rho_p L_p \frac{dV}{dt} = -Y_p(V), \tag{16}$$

$$\frac{dL_p}{dt} = -C_p, \text{ at } V_* \leq V < V_{hr}, \tag{17}$$

$$\frac{dL}{dt} = -(V - U), L_p = L \text{ at } V \geq V_{hr}. \tag{18}$$

Since there are no direct experimental data on dependence of VNZh alloy and 30HGSA steel yield on the appeared longitudinal stress σ_x , for determination of $Y_p(P)$ we will use the results of experiments on implementation of projectiles of these metals into sand (Tables 2, 3). Dependence of yield on the velocity is defined with expression (8), evaluation of the strengthening coefficient is performed as per approximation of the experimental dependence of the relative penetration coefficient on initial implementation velocity $K(V_0)$ (formula (10)) with averaged parameters of sandy soil (Table 4).

As shown in [4], for copper rod the relative penetration coefficient is almost constant during penetration, at least in hydrodynamic stage and in plastic stage at $V > V_p$. For this coefficient stationarity check let's group the experiments with projectiles of strong materials (30HGSA steel and VNZh alloy (Tables 2, 3)) by close initial implementation velocities.

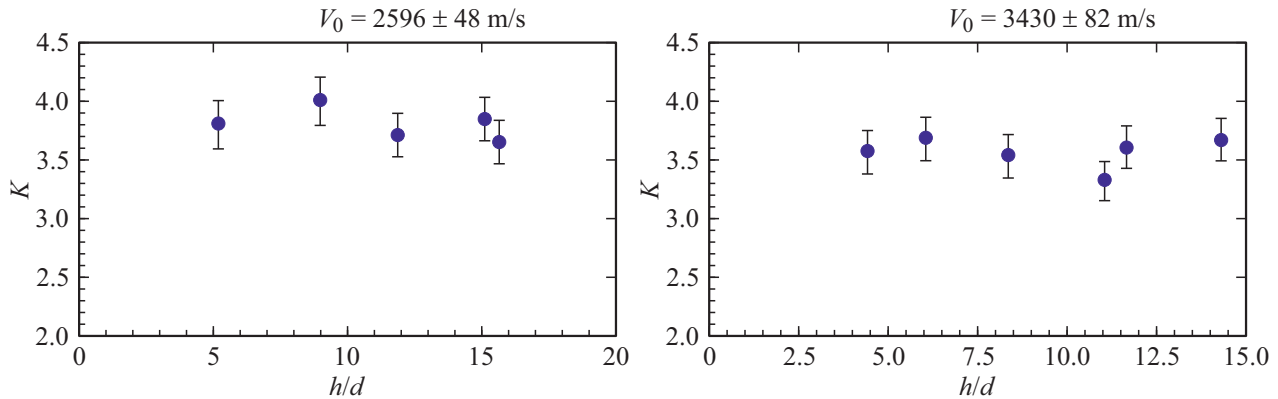


Figure 7. Dependence of relative penetration coefficient on depth of penetration into sand for projectile of VNZh90 alloy. ■ — experiment (Table 3, scatter $\pm 5\%$).

Two groups of experiments at average initial implementation velocity were allocated for each of both metals:

$V_0 = (1.953 \pm 0.022$ and 2.325 ± 0.046 km/s) — for 30HGSA steel;

$V_0 = (2.596 \pm 0.04848$ and 3.430 ± 0.082 km/s) — for VNZh alloy.

At close initial implementation velocities V_0 in different experiments (scatter from average value is 3% maximum) the penetration depth, on which the relative penetration coefficient was recorded, was significantly different.

Figures 6 and 7 show the diagrams of experimental dependence of relative penetration coefficient on penetration depth for projectile of 30HGSA steel and VNZh alloy. In the first approximation the relative penetration coefficient, defined at various depths, for this average implementation velocity can be considered constant within the experimental error $\pm 5\%$. Therefore, each value of K , presented in Tables 2 and 3 for certain value of h and current value of V , can be assigned both to h_0 , and V_0 .

For each metal the experimental dependence $K = f(V_0)$, that is approximated with analytical dependence (12), is defined. As per this approximation, considering expressions (14) and (8), using the least squares method the value of strengthening coefficient k of individual metal is defined. Approximated dependencies for VNZh alloy and 30HGSA steel are presented in Figs. 8 and 9, while the observed values of the strengthening coefficients k — in Table 4.

For 30HGSA steel at implementation velocity of 2.325 km/s only two experiments are presented, but, based on experiments with other velocity, including with projectile of VNZh alloy, there are no reasons to be skeptical on stationarity of the relative penetration coefficient.

5. Results of calculations as per IMHT for penetration of metal rods into sand

Tables 1–3 include initial data, at which the experiments and calculations as per IMHT were performed. Calculations of penetration of the examined projectiles into sand were

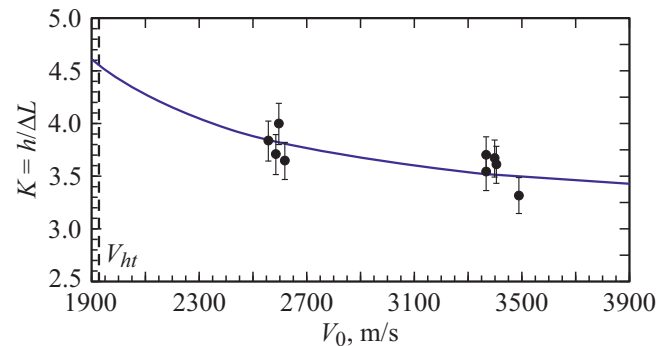


Figure 8. Dependence of the coefficient of relative penetration into sand for the rod of VNZh alloy. ● — experiment (Table 3, scatter $\pm 5\%$), — — approximation with analytical dependence (12), $Y_p = Y_p(V)$ considering (14) and (8) with coefficient $k = 0.25$, $Y_* = 1.775$ GPa.

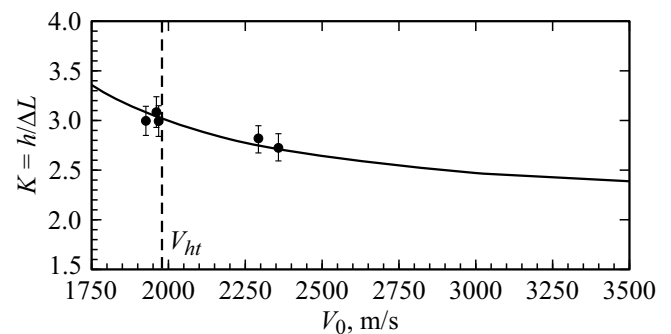


Figure 9. Dependence of the coefficient of relative penetration into sand for the rod of 30HGSA steel: ● — experiment (Table 2, scatter $\pm 5\%$), — — approximation with analytical dependence (12), $Y_p = Y_p(V)$ considering (14) and (8) with coefficient $k = 0.175$, $Y_* = 1.34$ GPa.

performed as per the system of equations (1), (2), (5), (8), (15)–(18) with specified initial data, specifically

- values of Y_* , C_p , V_0 , k ;
- sandy soil parameters (C_x , ρ_t);
- metal rods parameters (m , d , L_0 , ρ_p).

Table 5. Values of characteristic velocities of projectiles penetration into sand

Projectile material, soil parameters	V_* , km/s (experiment)	V_p , km/s	V_{ht} , km/s formula (5)	V_{sht} , km/s
Copper M1 ($\rho_t = 1.7 \text{ g/cm}^3$, $C_x = 1.5$, $Y_* = 0.320 \text{ GPa}$, $k = 0.13$)	0.500	0.850	1.530	2.100
VNZh alloy ($\rho_t = 1.7 \text{ g/cm}^3$, $C_x = 1.75$, $Y_* = 1.775 \text{ GPa}$, $k = 0.25$)	1.092	2.500	1.930	3.400
30HGSA steel ($\rho_t = 1.8 \text{ g/cm}^3$, $C_x = 1.5$, $Y_* = 1.34 \text{ GPa}$, $k = 0.175$)	0.996	2.550	1.980	3.500

Value of shortening of the hard projectile part ΔL_p due to plastic deforming was defined only for copper projectile. The following columns of the Tables 1–3 contain values, calculated as per IMHT. Comparison with the experiment was performed for fixed values of V_0 and h . Tables also contain the experimental values of the deforming coefficient $K_p = h/\Delta L$ (in plastic stage for copper rod) and relative penetration coefficient $K = h/\Delta L$ for both penetration stages. Difference of the calculated values of t , ΔL , K for three projectile materials and ΔL_p , K_p for copper projectile from the experimentally observed values was 5–10% maximum.

Table 5 includes calculated values of velocities V_* , $V + p$, V_{ht} and V_{sht} for implementation of projectiles of three examined materials into sand (value of V_* is calculated as per formula (2), according to value of Y_* (Table 4), that define the characteristic velocity ranges, within which the depth of completion of deforming qualitatively differs.

Calculations for strong metals — VNZh alloy and 30HGSA steel, as well as for copper M1 [4], have showed the presence of four characteristic ranges of penetration velocity:

Range I ($V_* \leq V_0 < V_{ht}$): projectile, deforming plastically, without reaching the complete plastic compression, maintains the hard residue from its initial length.

Range II ($V_{ht} \leq V_0 < V_p$): projectile has a triple deforming structure (hydrodynamic actuation + plastic deforming + hard residue).

Range III ($V_p \leq V_0 < V_{sht}$): projectile deforms in two modes (hydrodynamic actuation + complete plastic deforming).

Range IV ($V_0 \geq V_{sht}$): projectile completely actuates hydrodynamically.

Complete plastic compression or hydrodynamic actuation is implemented at range III and IV velocities only.

In case of stationarity of the deforming coefficient K_p the depth of completion of deforming in plastic stage can be evaluated as

$$H = K_p \cdot \Delta L_p, \tag{19}$$

and in case of stationarity of the relative penetration coefficient K the depth of complete actuation (depth of penetration in hydrodynamic mode) can be evaluated as

$$H = K \cdot \Delta L. \tag{20}$$

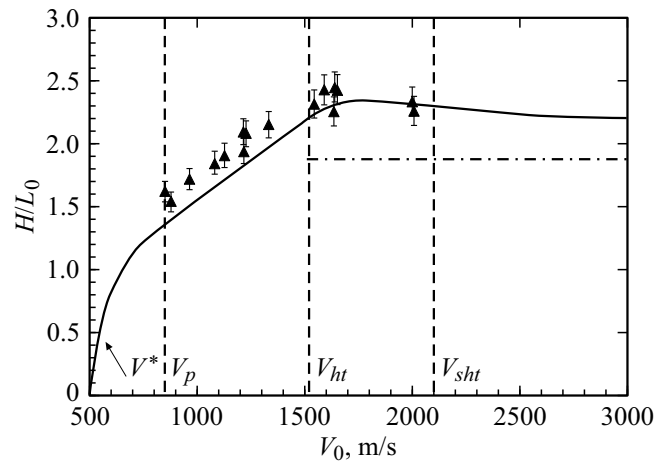


Figure 10. Depth of completion of deforming of the projectile of copper M1 at penetration into sand [4]. — calculation as per IMHT ($\rho_t = 1.7 \text{ g/cm}^3$, $C_x = 1.5$); \blacktriangle — experiment (Table 1, scatter $\pm 5\%$); - - - - - evaluation as per formula of M.A. Lavrentiev (17).

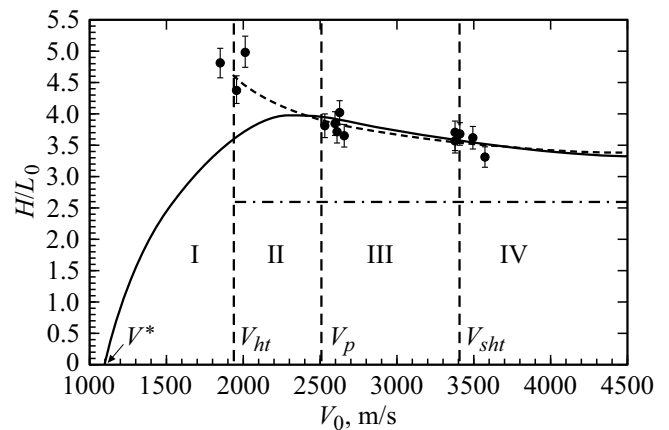


Figure 11. Depth of completion of deforming of the projectile of VNZh alloy at penetration into sand: dotted line — formula (12); — calculation as per IMHT ($\rho_t = 1.7 \text{ g/cm}^3$, $C_x = 1.75$); \bullet — experiment (Table 3, scatter $\pm 5\%$); - - - - - evaluation as per formula of M.A. Lavrentiev (21).

Figures 10–12 contain the diagrams of calculation as per IMHT of the depth of deforming completion of projectiles of three examined materials (current velocity

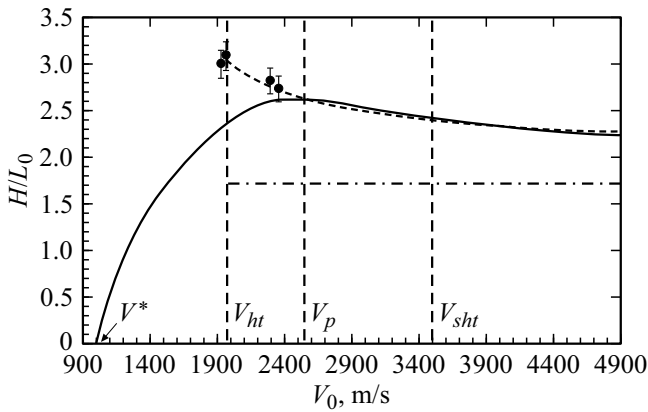


Figure 12. Depth of completion of deforming of the projectile of 30HGSA steel at penetration into sand. Dotted line — formula (12); — — calculation as per IMHT ($\rho_t = 1.8 \text{ g/cm}^3$, $C_x = 1.5$), • — experiment (Table 2, scatter $\pm 5\%$); - - - - evaluation as per formula of M.A. Lavrentiev (21).

$V > V_*$) at penetration into sand with parameters from Table 5. Experimental relative penetration coefficient (in case of stationarity) defines the dimensionless full depth of penetration in hydrodynamic mode. In case of copper projectile at $V_{ht} > V_0 \geq V_p$ the experimental deforming coefficient K_p can define the depth of deforming completion (but not the full depth of penetration) for plastic penetration stage. Calculated deforming coefficient K_p of copper projectile (see Fig. 5 [4]), considering rod braking with penetration depth, will decrease (even at $V \geq V_p$ within 5–7%) and correspondingly the calculated depth of deforming completion will be somewhat less than the value of the experimental K_p .

Vertical dashed lines on diagrams of Figs. 10–12 designate the velocities of four ranges boundaries (Table 5): hydrodynamic transition velocity V_{ht} , minimum velocity of the complete plastic compression V_p and minimum velocity of complete hydrodynamic actuation V_{sh} . Critical velocity V_* is also shown on the diagrams. Horizontal dashed lines on diagrams correspond to hydrodynamic coefficient of M.A. Lavrentiev considering the resistance coefficient C_x (values are presented in Table 5):

$$K = \sqrt{\rho_p / (\rho_t C_x)}. \tag{21}$$

For VNZh alloy and 30HGSA steel the experimental values of the relative penetration coefficient K , corresponding to the plastic mode of projectile deforming (to the left from the hydrodynamic transition boundary), can not define the depth of deforming completion (let alone the full penetration depth). For these implementation velocities ($V_0 < V_{ht}$) the depth of deforming completion defines the deforming coefficient K_p (formula (6)), that is less than K (in case of plastic metals — significantly less), but in experiments with projectiles of VNZh allot and 30HGSA steel it was not defined. As was shown above, only at

implementation velocities $V_0 \geq V_p$ the stationarity of both coefficients K and K_p can be safely stated (maximum change over the whole depth does not exceed 5%).

6. Empirical formula of the relative penetration coefficient

Dependence of the relative penetration coefficient on dimensionless initial velocity $\tilde{V} = V_0/V_*$ can be described with a single relatively simple empirical dependence

$$K(\tilde{V}) = \frac{1}{\mu} \sqrt{\frac{1}{b}} \left[1 + \frac{1}{\sqrt{\tilde{V}^2 - 1}} \right], \tag{22}$$

which can be derived from expansion of expression under integral sign of formula (13) at $V_0 \rightarrow V_*$: within the limit it can be assumed, that $U_0 = V_0$ and that the strengthening coefficient $k = 0$, then

$$\sqrt{\frac{1}{1 - \frac{2Y_p(V_0)}{C_x \rho_t U_0^2}}} = \sqrt{\frac{1}{1 - \frac{2 \cdot 0.5 C_x \rho_t V_*^2}{C_x \rho_t V_0^2}}} \rightarrow \left[1 + \frac{1}{\sqrt{\tilde{V}^2 - 1}} \right]. \tag{23}$$

Figure 13 shows the experimental values of the relative penetration coefficient K , multiplied by the value of $\mu = \sqrt{\rho_t / \rho_p}$, depending on $\tilde{V} = V_0/V_*$, compared to type approximation (23).

Using the approximation of experimental data, corresponding to hydrodynamic projectile actuation mode, we get the value of parameter $b = 1.5 \pm 0.025$. For copper projectile the experimental data, corresponding to implementation velocity $V > V_p$ ($\tilde{V} = 1.7$), were used, since at this velocity the relative penetration coefficient can be considered stationary. Value of parameter b is equal to average resistance coefficient of projectile with flat front face at penetration into sandy soil of average density $\rho_t = 1.7 \text{ g/cm}^3$ and moisture $W = 10\%$, that was used in

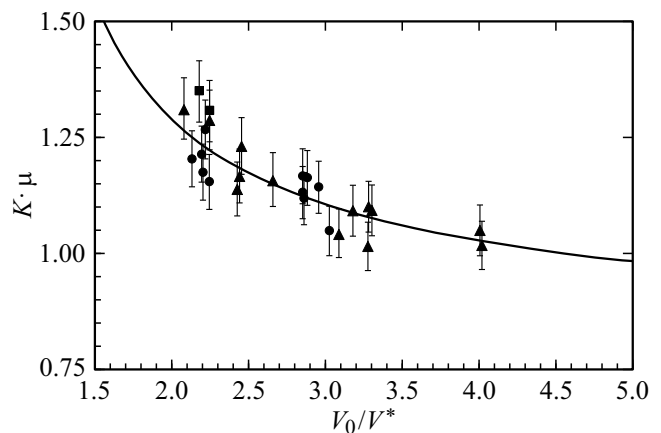


Figure 13. Standardized relative penetration coefficient. — — formula (22) ($\mu = \sqrt{\rho_t / \rho_p}$); • — experiment: projectile of VNZh alloy (Table 3, scatter $\pm 5\%$); ▲ — experiment, projectile of copper M1 (Table 1, scatter $\pm 5\%$); ■ — experiment, projectile of 30HGSA steel (Table 2, scatter $\pm 5\%$).

the most of our experiments. The approximating curve on diagram (Fig. 13) is a function (18) with $b = C_x = 1.5$.

Conclusion

Results of calculations on improved modified hydrodynamic theory of Alekseevskii–Tate (IMHT) are in good agreement with experiment data, observed at high-velocity penetration (impact velocity V_0 is from 0.5 to 3.5 km/s) into sandy soil for projectiles made of three different metals: copper M1, VNZh alloy and 30HGSA steel.

Using IMHT and experimental data on dependence of the relative penetration coefficient K (relation of penetration depth to the length of worn projectile part) on implementation velocity, it is possible to define the strengthening coefficient k in linear dependence of projectile material yield on implemented pressure.

At penetration in hydrodynamic projectile actuation mode the relative penetration coefficient K can be approximated with dependence only on relation of initial implementation velocity to critical velocity, in exceeding of which the penetration happens with plastic deforming of the projectile. Value of critical velocity for individual values of projectile material density, sandy soil density and moisture can be different.

Conflict of interest

The authors declare that they have no conflict of interest.

References

- [1] M.V. Kaminskij, G.F. Kopytov, V.A. Mogilev, Yu.F. Travov, Yu.I. Faikov. PMTF, **51** (3), 32 (2010) (in Russian).
- [2] V.P. Alekseevskii. FGV, **2**, 99 (1966) (in Russian).
- [3] A. Tate. Sb. perevodov „Mekhanika“, **5**, 125 (1968) (in Russian).
- [4] A. Tate. J. Mech. Phys. Solids., **17** (3), 141 (1969).
- [5] G.F. Kopytov, V.A. Mogilev, A.P. Snopkov. Izv. RAN, **4** (49), 31 (2006) (in Russian).
- [6] A. Tate. Int. J. Mech. Sci., **19** (2), 121 (1977).
- [7] R.F. Recht. Int. J. Enging. Sci., **16**, 809 (1978).
- [8] A. Tate. Int. J. Mech. Sci., **28** (9), 599 (1986).
- [9] S.I. Gerasimov, D.V. Zakharov, A.V. Zubankov, V.A. Kikeev, E.S. Khoroshajlo. Nauchnaya vizualizatsiya, **10** (2), 1 (2018) (in Russian). DOI: 10.26583/sv.10.2.10
- [10] V.A. Berdnikov, M.V. Kaminskij, Yu.G. Kiselev, G.F. Kopytov, V.A. Mogilev, Yu.F. Travov, Yu.I. Faikov, Yu.A. Fateev. *Ekspperimental'noe issledovanie dvizheniya konusov i tsilindra v peschanoj srede. Sbornik materialov II-oj nauchnoj konferentsii RARAN „Sovremennye metody proektirovaniya i otrabotki raketno-artillerijskogo vooruzheniya“*. (RFYAC-VNIIEF, Sarov, 2002), p. 276–279 (in Russian).
- [11] Yu.V. Bat'kov, B.L. Glushak, S.A. Novikov. FGV, **25** (5), 126 (1989) (in Russian).
- [12] L.P. Orlenko (red.). *Fizika vzryva* (Fizmatlit, M., 2004), V. 2 (in Russian).
- [13] M.A. Lavrentiev. UMN, **4**, 41 (1957) (in Russian).
- [14] S.I. Gerasimov, V.I. Erofeev, Yu.F. Travov, A.G. Ioilev, V.V. Pisetsky, A.P. Kalmykov, S.A. Kapinos, N.V. Lapichev. ZhTF, **91** (3), 542 (2021) (in Russian). DOI: 10.21883/JTF.2021.03.50535.233-20
- [15] S.I. Gerasimov, V.I. Erofeev, E.G. Kosyak, V.A. Kikeev, V.V. Pisetsky. ZhTF, **90** (8), 1374 (2020) (in Russian). DOI: 10.21883/JTF.2020.08.49550.365-19
- [16] S.I. Gerasimov, V.I. Erofeev, A.V. Zubankov, V.A. Kikeev, V.V. Pisetsky. IFZh, **94** (1), 174 (2021) (in Russian).
- [17] I.S. Grigor'ev, E.Z. Mejlikhov (red.). *Fizicheskie velichiny, spravochnik*. (Energoatomizdat, M., 1991) (in Russian).